

# Measurements of $\Delta G$ at COMPASS

Konrad Klimaszewski (on behalf of the COMPASS collaboration)

The Andrzej Soltan Institute for Nuclear Studies, Warsaw

**Abstract.** The direct measurement of the gluon polarisation in the nucleon at the COMPASS experiment is discussed. Three complementary analyses are considered. All of them study  $\Delta G/G$  using method based on selection of events originating from the Photon Gluon Fusion process. Most precise preliminary value of  $\Delta G/G$  is obtained from the high  $p_T$  pair channel for the  $Q^2 < 1$  (GeV/c)<sup>2</sup> region:  $\frac{\Delta G}{G} = 0.016 \pm 0.058(stat.) \pm 0.055(syst.)$ .

## 1 Introduction

One of the main goals of the COMPASS experiment [1], is the study of nucleon spin structure. Still after over 30 years of experimental and theoretical effort there are a lot of questions to be answered.

In the frame of the Quark Parton Model the nucleon spin is described by a sum rule:

$$\frac{1}{2} = \frac{1}{2}\Delta\Sigma + \Delta G + L_q + L_g, \quad (1)$$

where the  $\Delta\Sigma$  is a contribution from helicities of quarks, the  $\Delta G$  a contribution from helicities of gluons and  $L_{q,g}$  orbital momenta of quarks and gluons, respectively. A value of  $\Delta\Sigma$  was measured by the EMC experiment [2,3]. In following years obtained result was confirmed by several experiments [4–6]. All results indicate that  $\Delta\Sigma$  is smaller than expected from naive Quark Parton Model and cannot account for the whole spin of the nucleon. Recent results show that the value of  $\Delta\Sigma$  is close to 30%, *e.g.*  $\Delta\Sigma = 0.30 \pm 0.01(stat.) \pm 0.02(evol.)$  [6]. Therefore it is clear that the rest of the nucleon spin originates from polarised gluons and orbital motion of partons in the nucleon. The COMPASS experiment aims to directly measure the gluon polarisation to shed new light on the “nucleon spin puzzle”. The measurement is performed using cross-section asymmetries for Photon Gluon Fusion (PGF) events in the Deep Inelastic Scattering (DIS) of leptons on nucleons and probes  $\Delta G$  in the region of  $x_g \simeq 0.1$ .

## 2 Experimental setup

In the COMPASS experiment interactions of polarised muons with polarised deuterons are studied. The muon beam is obtained from the SPS accelerator at CERN. A proton beam accelerated in the SPS to 400 GeV/c interacts with a beryllium target forming a  $\pi^\pm$  beam. Pions fly through a decay pipe where muons are produced:  $\pi \rightarrow \mu + \nu_\mu$ . This tertiary beam is directed through an absorber where leftover hadrons are filtered out. Finally using a set of magnets beam is focused and its charge and momentum selected.

The muon beam is naturally polarised due to the parity-violating decay of the pion. In pion rest frame outgoing muons are polarised in 100%. In laboratory frame the polarisation of muons depends on the ratio between pion and muon momenta:

$$P_\mu = \frac{m_\pi^2 + (1 - 2E_\pi/E_\mu)m_\mu^2}{m_\pi^2 - m_\mu^2}. \quad (2)$$

Careful selection of pion and muon energies enables us to obtain a highly polarised muon beam [7]. COMPASS is working with a  $\mu^+$  beam of 160 GeV/c momentum and a polarisation  $P_B \simeq 80\%$ .

As target material we are using  ${}^6\text{LiD}$ . It provides good compromise between the dilution factor  $f \simeq 0.4$  and the achieved polarisation  $P_T \simeq 50\%$ . The target is composed of two cells - each 60 cm long, which are placed along the beam. The cells are oppositely polarised: parallel and anti-parallel to the muon polarisation. Such setup enables us to measure both configurations simultaneously, this allows for cancellation of the beam flux in asymmetry calculation. A high polarisation is achieved using the Dynamic Nuclear Polarisation [8] for this the target is kept under a very low temperature  $T = 0.5\text{K}$  and in a strong magnetic field of 2.5 T. Then the target is exposed to Micro Wave (MW) radiation of the energy needed to perform simultaneous spin flips of protons and electrons. This energy depends on the spin of the final state of e-p system (0, 1). So by choosing the proper MW energy we can perform flip only to one selected state. The electron almost immediately relaxates to a lower energy state. Due to its small magnetic moment the proton has small probability to change its spin orientation. This leads to buildup of the polarisation. The achieved relaxation times are of  $\sim 1000$  hours.

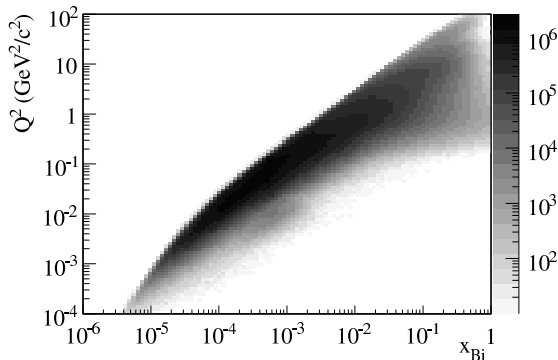


**Fig. 1.** Kinematic region covered by the COMPASS spectrometer.

Products of DIS of muons on nucleons are measured in a two stage spectrometer. The first part is dedicated to measure large angle tracks. The second one measures small angle tracks. Both stages of the spectrometer are equipped with a bending magnet used for momentum determination, electron and hadron calorimetry and various trackers. The spectrometer consist of  $\sim 250$  tracking planes of various types: Silicon Microstrips, Scintillating Fibres, Proportional Chambers, Drift Chambers, Straws, GEMs and MicroMegas. Gas Electron Multipliers (GEMs) and Micro Mesh Gaseous detectors (MicroMegas) were used for the first time for such large scale experiment and in such high luminosity conditions. Particle Identification (PID) is provided by a Ring Image Cherenkov (RICH) detector. It enables us to separate  $\pi$ ,  $K$  and  $p$  for momenta from 2.5, 9, 17 GeV/c up to 50 GeV/c, respectively. PID is also provided by calorimetry and muon filters. The trigger system is based on scintillator hodoscopes and energy deposition in calorimeters. The kinematic region covered by the spectrometer is presented on fig. 1. More information about the COMPASS experimental setup can be found in Ref. [1].

### 3 Experimental asymmetry

We can define a counting asymmetry as  $A_{exp} = \frac{N^{\uparrow\downarrow} - N^{\uparrow\uparrow}}{N^{\uparrow\downarrow} + N^{\uparrow\uparrow}}$ , where  $N^{\uparrow\downarrow(\uparrow\uparrow)}$  are number of events with nucleons polarised anti-parallel (parallel) to muon spin direction. In the experiment we are using two target cells polarised oppositely. This allows for simultaneous measurement of both configurations with the same beam flux. Due to that the flux will cancel out in the asymmetry calculation. Such experimental setup means that the cells have different geometrical acceptance. In order to eliminate the acceptance effects polarisation of the target cells is reversed frequently (every 8 hours). Spin reversal is obtained by rotating the magnetic field. To cope with the dependence of the apparatus performance on the direction of the magnetic field of the target

magnet, Micro Wave reversal is performed ~every month. Taking the spin reversal into account we can rewrite the asymmetry in a new form:

$$A_{exp} = \frac{1}{2} \left( \frac{N^U - N^D}{N^U + N^D} + \frac{N'^D - N'^U}{N'^D + N'^U} \right), \quad (3)$$

where  $N^{U(D)}$  is a number of events originating from upstream (downstream) target cell and  $N'^{U(D)}$  a number of events originating from upstream (downstream) target cell after the field reversal.

Raw counting asymmetry can be related to cross-section asymmetry by

$$A_{||} = f P_T P_B A_{exp}, \quad (4)$$

where  $f$  is the dilution factor,  $P_T$  the target polarisation and  $P_B$  the beam polarisation. To decrease statistical errors a weighting method of asymmetry extraction is used [9]. In this method a weight  $w = f D P_B$  is applied on event by event basis instead of using average values. Thus, we finally obtain the following formula for the asymmetry:

$$\frac{A_{||}}{D} = \frac{1}{2 |P_T|} \left( \frac{\Sigma w_U - \Sigma w_D}{\Sigma w_U + \Sigma w_D} + \frac{\Sigma w'_D - \Sigma w'_U}{\Sigma w'_D + \Sigma w'_U} \right) \quad (5)$$

$$\delta \left( \frac{A_{||}}{D} \right) = \frac{1}{2 |P_T|} \sqrt{\frac{1}{\Sigma w_U^2 + \Sigma w_D^2} - \frac{1}{\Sigma w'_U^2 + \Sigma w'_D^2}}, \quad (6)$$

where  $D$  is the depolarisation factor,  $\Sigma w_{U(D)}$  a sum of weights for events originating from the upstream (downstream) target cell and  $\Sigma w'_{U(D)}$  is a sum of weights for events originating from the upstream (downstream) target cell after the field reversal.

#### 4 $\Delta G/G$ from scaling violations

To good approximation the muon-nucleon cross-section asymmetry  $A_{||}$  is related to the photon-nucleon cross-section asymmetry  $A_1$  by  $A_{||} = A_1 D$ , where  $D$  is the depolarisation factor. It can be also shown that  $A_1 \approx \frac{g_1}{F_1}$ , where  $g_1 = \sum e_i^2 q_i^+ - \sum e_i^2 q_i^-$  is the spin dependent structure function and  $F_1 = \sum e_i^2 q_i^+ + \sum e_i^2 q_i^-$  the spin independent structure function (well known from unpolarised experiments). In pQCD we can write:

$$g_1(x, Q^2) = \frac{1}{2} \langle e^2 \rangle \left[ C_q^S \otimes \Delta \Sigma + C_q^{NS} \otimes \Delta q^{NS} + 2n_f C_g \otimes \Delta G \right], \quad (7)$$

where  $C_i$  are the Wilson coefficients and  $\Delta q^{NS}(x, Q^2) = \sum_i (e_i^2 / \langle e_i^2 \rangle - 1) \Delta q_i(x, Q^2)$  are the nonsinglet polarised quark distributions.

We see that there is a contribution of gluons. Thus, by measuring  $g_1$   $\Delta G/G$  can be extracted. As seen from eq. 7  $g_1$  is composed of Parton Distribution Functions (PDFs) in the nucleon. The dependence of PDFs on the  $Q^2$  is described by the DGLAP evolution equations. The  $x$  (Bjorken variable) dependence is parametrised with a functional form, *e.g.*  $f(x) = \eta \frac{x^\alpha (1-x)^\beta (1+\gamma x)}{\int_0^1 x^\alpha (1-x)^\beta (1+\gamma x) dx}$ , where  $\alpha, \beta, \eta, \gamma$  are free parameters which are obtained from a fit to the experimental data. Usually  $g_1$  measurements are taken at different  $Q^2$  values. In the fit procedure this is accounted for by evolving  $g_1$  parametrisation to the  $Q^2$  of the data points, from the  $Q_0^2$  of the initial parametrisation. For each point contribution to  $\chi^2$  is calculated. The parameters are varied in such a way to minimise the total  $\chi^2$ . As a result we obtain parametrisations of PDFs from which first moments of the quark  $\Delta \Sigma(x)$  and the gluon  $\Delta G(x)$  contributions can be extracted. Current data indicate that  $\Delta \Sigma$  is about 0.3, where  $\Delta G$  is poorly constrained and it is estimated to be  $|\Delta G| < 0.3$  [6].

## 5 Direct measurement of $\Delta G/G$

A direct measurement of the gluon polarisation in the nucleon can be performed using events originating from the PGF process. In this process the virtual photon emitted by the incoming lepton interacts with a gluon coming from a nucleon. The photon retains part of the lepton polarisation, this provides us with a probe to sample the polarised gluons in the nucleon.

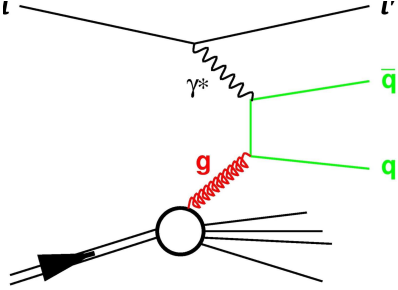


**Fig. 2.** The Photon Gluon Fusion process.

Here  $A_{||}$  is the cross-section asymmetry for scattering of leptons on nucleon target taking into account all available processes in LO pQCD.

$$A_{||} = \frac{\sigma^{\uparrow\downarrow} - \sigma^{\uparrow\uparrow}}{\sigma^{\uparrow\downarrow} + \sigma^{\uparrow\uparrow}} = \frac{\Delta\sigma}{\sigma} \quad (8)$$

Factorisation allows us to decompose the polarised and unpolarised cross-sections into:

$$\Delta\sigma = \Delta F \otimes \Delta\hat{\sigma} \otimes \tilde{D}; \quad \sigma = F \otimes \hat{\sigma} \otimes \tilde{D}$$

where  $\Delta F$ ,  $F$  are the polarised and unpolarised PDFs ( $\Delta G$ ,  $\Delta q$ ,  $G$ ,  $q$ ),  $\Delta\hat{\sigma}$ ,  $\hat{\sigma}$  the polarised and unpolarised partonic cross-sections and  $\tilde{D}$  the fragmentation function which we assume to be spin independent, so it will cancel out in asymmetry calculation.

We can rewrite the asymmetry in following form:

$$A_{||} = \sum_i R_i \langle \hat{a}_{LL}^i \rangle \frac{\Delta G}{G} + \sum_k R_k \langle \hat{a}_{LL}^k \rangle \frac{\Delta q}{q}, \quad (9)$$

where  $R_i$ ,  $R_k$  are the fractions of processes probing gluons in the nucleon (*e.g.* PGF) and processes probing quarks, respectively. The partonic cross-section asymmetry is defined by  $\hat{a}_{LL} = \frac{\Delta\hat{\sigma}}{\hat{\sigma}}$ . From this equation using measured value of  $A_{||}$ ,  $\Delta G/G$  can be extracted.

## 6 $\Delta G/G$ measurement at COMPASS

From eq. 9 it is clear how to extract  $\Delta G/G$  from PGF events. These events have to be selected, from background originating from other processes. In COMPASS this is performed using two channels. The first one so called “golden channel” is open charm production [10,11]. As there are no background processes in this channel it is theoretically very clean. It’s main disadvantage is low statistics.

The second one is “high  $p_T$  hadron pairs” channel [12]. Here we are looking for two hadrons in the final state, with high transverse momentum with regards to virtual photon. This channel provides us with large statistics. Unfortunately there is considerable contribution of background processes. This leads to theoretical uncertainties as we have to disentangle the different contributions.

### 6.1 Open charm production

In this analysis we are looking for  $D^0$  mesons in the final state. As the fraction of  $c$  quarks in the nucleon is negligible, all such hadrons (in LO of pQCD) will originate from the PGF process. Also, charm mass provides us with a hard scale that ensures factorisation. As there are no competing processes, this channel is theoretically very clean. It’s main disadvantage is low statistics.

We are searching for  $D^0$  in two channels:

$$\begin{aligned} c \rightarrow D^0 &\rightarrow K^+ \pi^- + cc \\ c \rightarrow D^{*+} (2010) &\rightarrow D^0 \pi_{slow}^+ \rightarrow K^- \pi^+ \pi_{slow}^+ + cc \end{aligned}$$

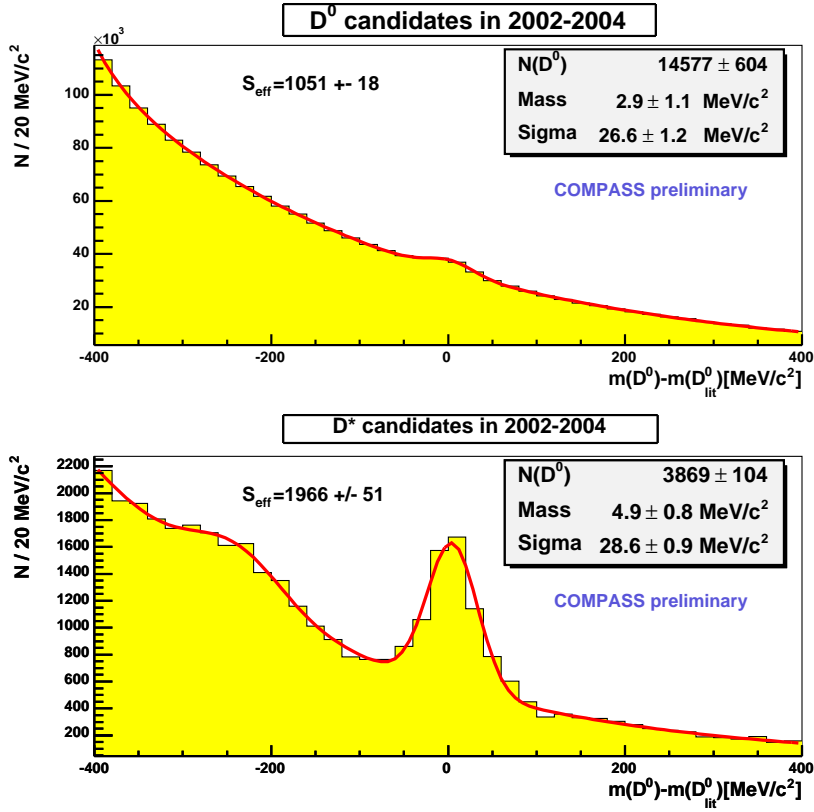


**Fig. 3.**  $D^0$  peak in  $K\pi$  invariant mass distribution for  $D^0$  channel (top) and  $D^*$  tagged channel (bottom) based on data collected in 2002-2004 years. A bump which shows up at low mass in  $D^*$  case is attributed to  $D^0 \rightarrow K\pi\pi^0$ . It is not included in S count.

In order to obtain a high luminosity we are forced to use a large target. Due to multiple scattering in the target material it is impossible to distinguish the primary vertex from the  $D^0$  decay vertex and we are left with a high combinatorial background. In order to suppress it, kaon identification provided by our RICH detector is essential. In addition, to further suppress the background kinematic cuts are applied. The fraction of the virtual photon energy carried by the  $D^0$  and the angle between direction of  $D^0$  and kaon in  $D^0$  centre of mass system are demanded to be large enough:  $z_{D^0} \gtrsim 0.25$  and  $-\cos\Theta_K^* \gtrsim 0.5$ .

The resulting  $D^0$  signal is presented in fig. 3. The effective signal is defined as  $\frac{S^2}{S+B}$ , where the signal S and the background B are estimated from the area under the fit to the mass distribution. Still, the level of background is very high. Thus, a more efficient tagging method is considered.

Looking for  $D^0$  mesons coming from  $D^*$  decays is such a method. The difference between  $D^*$  and  $D^0$  mass is very small. This leads to a fact that the pion coming from the  $D^*$  decay has low energy and is called a slow pion. Those characteristic of this process are an efficient tagging signature as can be seen on fig. 4. The obtained  $D^*$  tagged  $D^0$  signal is presented on fig. 3. For  $D^*$  case slightly looser kinematics cuts are used:  $z_{D^0} \gtrsim 0.20$  and  $-\cos\Theta_K^* \gtrsim 0.85$ .

In case of open charm channel we can write the asymmetry in following form:

$$\frac{A_{||}}{D} = \frac{S}{S+B} \left\langle \frac{a_{LL}}{D} \right\rangle \frac{\Delta G}{G} \quad (10)$$

The ratio  $S/(S+B)$  is taken from the fit to invariant mass of  $D^0$  candidates in bins of  $a_{LL}$ . As we don't have full knowledge about kinematics of the event (only one D meson is

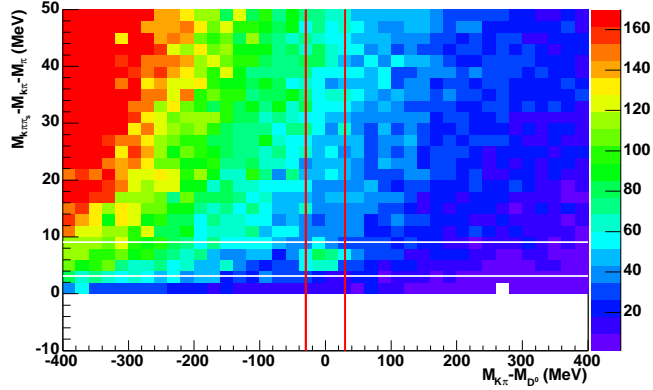


Fig. 4. The reconstructed mass difference between candidates for the  $D^*$  and  $D^0$ , reduced by nominal pion mass, is plotted versus  $M_{\pi K} - M_{D^0}$ . A signal is seen as expected around  $\Delta M - m_{\pi} \approx 6 \text{ MeV}/c^2$ .

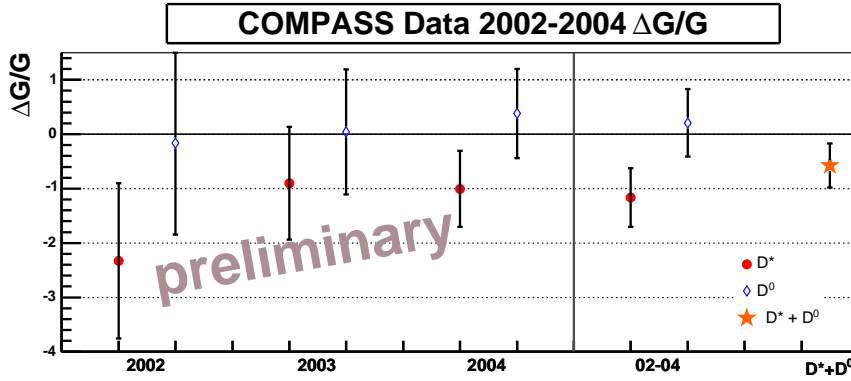


Fig. 5. Results for  $\Delta G/G$  for  $D^*$  tagged  $D^0$ s and untagged ones. Presented are values obtained for three years of data taking and a combined result.

reconstructed)  $a_{LL}$  has to be parametrised using measured observables. A parametrisation was prepared using Neural Networks (NN) and a Monte Carlo (MC) simulation, based on AROMA generator [13]. Obtained correlation factor between  $a_{LL}$  generated by MC and  $a_{LL}$  obtained from NN is  $c_F = 82\%$ .

In estimation of systematic error various sources of uncertainties were considered. The largest contributions to the systematic error come from: the background asymmetry, the false asymmetries and the fitting procedure. Other sources: MC tuning, parametrisations of beam polarisation, dilution and depolarisation factors. The combined systematic error is estimated to be 0.17.

The extracted values of  $\Delta G/G$  for both  $D^0$  and  $D^*$  channels are presented in fig. 5.

Finally the preliminary value obtained using data collected in 2002-2004 is

$$\frac{\Delta G}{G} = -0.57 \pm 0.41(\text{stat.}) \pm 0.17(\text{syst.})$$

at an average  $x_g \approx 0.15$  (RMS 0.8) and at a scale  $\approx 13(\text{GeV}/c)^2 (\approx 4m_c^2)$ .

## 6.2 High $p_T$ hadron pairs

In the LO of pQCD one should take into account 3 processes: the Leading Process (LP) where  $\gamma^*$  interacts with quark from nucleon, the QCD Compton (QCDC) process where we have

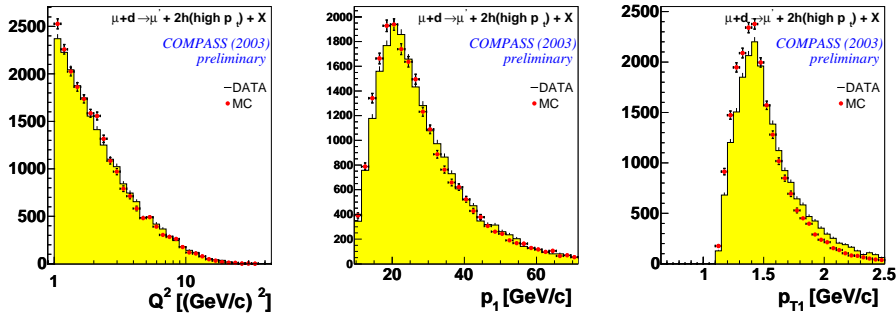


**Fig. 6.** Comparison of data and MC for high  $p_T$   $Q^2 > 1$  (GeV/c) $^2$  sample. Presented are the distributions of  $Q^2$  variable, momentum and transverse momentum of leading hadrons.

additional gluon radiation in the final state and the PGF. Hadron originating from LP can obtain  $p_T$  only from fragmentation or from intrinsic transverse momentum of the struck quark. This means that such hadrons will have rather small  $p_T$ . Thus by selecting high transverse momenta, fraction of LP in selected sample is greatly reduced.

In the high  $p_T$  hadron pair channel two complementary analyses are performed. One for the  $Q^2 > 1$  (GeV/c) $^2$  region and the second for  $Q^2 < 1$  (GeV/c) $^2$ . Such division originates from the regions of applicability of the two MC generators that are used: LEPTO [14] and PYTHIA [15].

The high  $p_T$  sample selection is based on a set of cuts. First at least two hadron tracks are required to be reconstructed in the primary vertex. Then to suppress the contribution from the the LP and in case of the  $Q^2 < 1$  (GeV/c) $^2$  sample ensure factorisation we require  $p_T$  of two fastest hadrons to be  $> 0.7$  GeV/c and their  $\sum p_T^2$  to be  $> 2.5$  (GeV/c) $^2$ . To remove regions with low sensitivity to  $\Delta G$  and regions with large radiative corrections we are selecting events where  $0.1 < y < 0.9$  in case of the  $Q^2 > 1$  (GeV/c) $^2$  sample and  $0.35 < y < 0.9$  in case of the  $Q^2 < 1$  (GeV/c) $^2$  sample. Finally to ensure that only events from current fragmentation region are selected and to remove  $\rho$  resonance three additional cuts are imposed:  $x_F, z > 0$  and  $M_{inv} > 1.5$  GeV/c.

### 6.2.1 The $Q^2 > 1$ (GeV/c) $^2$ sample

For this channel in LO of pQCD we can write the expression for  $A_{||}$  in following form:

$$\frac{A_{||}}{D} \simeq A_1 \left[ \left\langle \frac{a_{LL}^{LP}}{D} \right\rangle R_{LP} + \left\langle \frac{a_{LL}^{QCDC}}{D} \right\rangle R_{QCDC} \right] + \frac{\Delta G}{G} \left\langle \frac{a_{LL}^{PGF}}{D} \right\rangle R_{PGF} \quad (11)$$

where  $R_i$  - are the fractions of processes in the sample.

In first order approximation we neglect contributions from LP and QCDC. The value of  $a_{LL}$  is calculable in pQCD [16], but knowledge about exact parton kinematics is required. This means that values of  $a_{LL}$  and  $R_{PGF}$  have to be extracted from MC simulations. The fraction of the PGF process in the final sample was estimated to be  $R_{PGF} = 0.34 \pm 0.07$ .

It is obvious that a good agreement between data and MC is crucial. For the  $Q^2 > 1$  (GeV/c) $^2$  sample we are using the LEPTO MC generator to simulate  $\mu N$  scattering. For the simulation of the apparatus the GEANT3 framework [17] is used. fig. 6 presents the agreement between data and MC.

The preliminary value of  $\frac{\Delta G}{G} = 0.06 \pm 0.31(stat.) \pm 0.06(syst.)$  was obtained at  $\langle x_g \rangle = 0.13$  and at an average scale of 3 (GeV/c) $^2$ .

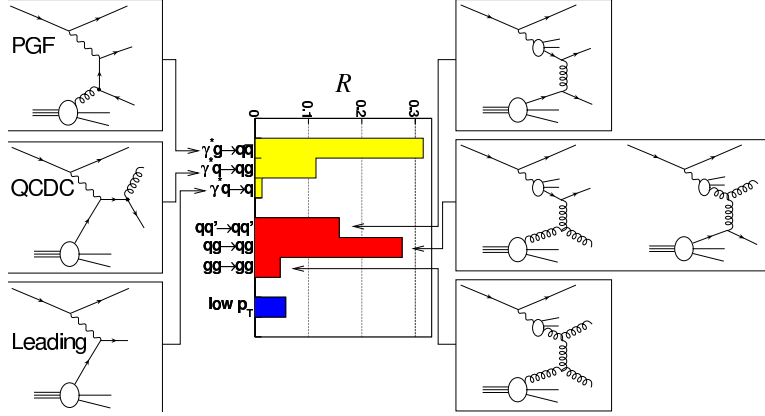


**Fig. 7.** Relative contributions  $R$  of the dominant PYTHIA processes to the MC sample of high  $p_T$  events at  $Q^2 < 1$   $(\text{GeV}/c)^2$ . Left: direct processes, right: resolved processes. Longitudinal photons, as well as minor resolved photon contributions, are not shown.

### 6.2.2 The $Q^2 < 1$ $(\text{GeV}/c)^2$ sample

In region of the  $Q^2 < 1$   $(\text{GeV}/c)^2$  there is additional contribution of resolved photon processes. In fig. 7 fractions of contributing processes are presented. They were estimated from a MC simulation using the PYTHIA MC generator. Three processes are treated as a signal: PGF and two resolved photon processes that probe gluons from the nucleon -  $gq$ ,  $gg$ , LP and so called “low  $p_T$ ” sample, which consists of nonperturbative processes are neglected as they contribute only small fraction of events. Taking all this into consideration leads us to following expression:

$$\begin{aligned}
 A_{||}/D &= R_{PGF} \left\langle \frac{a_{LL}^{PGF}}{D} \right\rangle \frac{\Delta G}{G} \\
 &+ R_{QCDC} \left\langle \frac{a_{LL}^{QCDC}}{D} \right\rangle A_1 \\
 &+ R_{qq} \left\langle \frac{a_{LL}^{qq}}{D} \right\rangle \frac{\Delta q}{q} \frac{\Delta q^\gamma}{q^\gamma} \\
 &+ R_{qg} \left\langle \frac{a_{LL}^{qg}}{D} \right\rangle \frac{\Delta q}{q} \frac{\Delta G^\gamma}{G^\gamma} \\
 &+ R_{gq} \left\langle \frac{q}{D} \right\rangle \frac{\Delta G}{G} \frac{\Delta q^\gamma}{q^\gamma} \\
 &+ R_{gg} \left\langle \frac{a_{LL}^{gg}}{D} \right\rangle \frac{\Delta G}{G} \frac{\Delta G^\gamma}{G^\gamma}
 \end{aligned} \tag{12}$$

where  $R_i$  is the fraction of process  $i$ ,  $a_{LL}^i$  is asymmetry [16] on partonic level (both  $R_i$  and  $a_{LL}^i$  are obtained from MC simulations),  $A_1$ ,  $q$ ,  $\Delta q$  are the parton distributions in the nucleon (taken from parametrisations to data [4, 18–20]),  $q^\gamma$ ,  $G^\gamma$  are unpolarised PDFs in the photon (also taken from parametrisation to data [21]) and  $\Delta q^\gamma$ ,  $\Delta G^\gamma$  are polarised PDFs in the photon (estimated using min-max scenario [22]). Terms in eq.12 that contribute to the signal are underlined.

Similarly to  $Q^2 > 1$   $(\text{GeV}/c)^2$  sample good agreement between data and MC is crucial. It is presented on fig. 8.

Using data collected in 2002–2003 years value of gluon polarisation is measured to be  $\frac{\Delta G}{G} = 0.024 \pm 0.089(\text{stat.}) \pm 0.057(\text{syst.})$  at  $x_g \approx 0.095_{-0.04}^{+0.08}$  (RMS 0.8). The scale at which measurement is made was estimated to be  $3(\text{GeV}/c)^2$ . This result was published [23]. Analysis

of combined data from years 2002-2004 provides us with a more precise preliminary result:

$$\frac{\Delta G}{G} = 0.016 \pm 0.058(\text{stat.}) \pm 0.055(\text{syst.})$$

This value was presented on several conferences.

## 7 Conclusions and outlook

On fig. 9 the results from the three channels are compared with the results from other experiments and with the result obtained from QCD fits of the  $g_1$  structure function. Within experimental uncertainties all results are compatible. We can conclude from them that the gluon polarisation is small in the region of  $x_g \simeq 0.1$  and the first moment of  $\Delta G$  is probably also small.

During a stop in 2005 the COMPASS spectrometer has undergone a major upgrade. The readout electronics and the internal optics were exchanged for the central part of RICH detector. New electromagnetic calorimeter was installed also new target solenoid magnet with larger aperture exchanged one inherited from the SMC experiment. Data taking was restarted in 2006 and provided a considerable gain in collected statistics. Analysis of 2006 data is ongoing. Other means of increasing available statistics are also considered *e.g* using Neural Networks as a tool for selecting PGF events.

If the gluon polarisation is indeed small it would be very interesting to measure contribution of orbital momentum of the partons to the nucleon spin. Such measurement using the Deeply Virtual Compton Scattering to access the Generalised Parton Distributions is considered for the COMPASS successor.

## References

1. P. Abbon et al. (COMPASS), Nucl. Instrum. Meth. **A577**, 455 (2007)
2. J. Ashman et al. (European Muon), Phys. Lett. **B206**, 364 (1988)
3. J. Ashman et al. (European Muon), Nucl. Phys. **B328**, 1 (1989)
4. B. Adeva et al. (Spin Muon), Phys. Rev. **D58**, 112002 (1998)
5. P.L. Anthony et al. (E155), Phys. Lett. **B493**, 19 (2000)
6. V.Y. Alexakhin et al. (COMPASS), Phys. Lett. **B647**, 8 (2007)
7. D. Adams et al. (Spin Muon), Phys. Rev. **D56**, 5330 (1997)
8. A. Abragam and M. Goldman, *Nuclear Magnetism: Order and Disorder* (Clarendon Press, Oxford, 1982)
9. E.S. Ageev et al. (COMPASS), Phys. Lett. **B647**, 330 (2007)
10. A.D. Watson, Z. Phys. **C12**, 123 (1982)
11. M. Gluck, E. Reya, Z. Phys. **C39**, 569 (1988)
12. A. Bravar, D. von Harrach, A. Kotzinian, Phys. Lett. **B421**, 349 (1998)
13. G. Ingelman, J. Rathsman, G.A. Schuler, Comput. Phys. Commun. **101**, 135 (1997)
14. G. Ingelman, A. Edin, J. Rathsman, Comput. Phys. Commun. **101**, 108 (1997)
15. T. Sjostrand, S. Mrenna, P. Skands, JHEP **05**, 026 (2006)
16. C. Bourrely, J. Soffer, F.M. Renard, P. Taxil, Phys. Rept. **177**, 319 (1989)
17. e.a. R. Brun, CERN-W5013 (1994), <http://consult.cern.ch/writeups/geant>
18. K. Abe et al. (E143), Phys. Rev. **D58**, 112003 (1998)
19. M. Gluck, E. Reya, M. Stratmann, W. Vogelsang, Phys. Rev. **D63**, 094005 (2001)
20. M. Gluck, E. Reya, A. Vogt, Eur. Phys. J. **C5**, 461 (1998)
21. M. Gluck, E. Reya, I. Schienbein, Phys. Rev. **D60**, 054019 (1999)
22. M. Gluck, E. Reya, C. Sieg, Eur. Phys. J. **C20**, 271 (2001)
23. E.S. Ageev et al. (COMPASS), Phys. Lett. **B633**, 25 (2006)
24. B. Adeva et al. (Spin Muon), Phys. Rev. **D70**, 012002 (2004)
25. A. Airapetian et al. (HERMES), Phys. Rev. Lett. **84**, 2584 (2000)

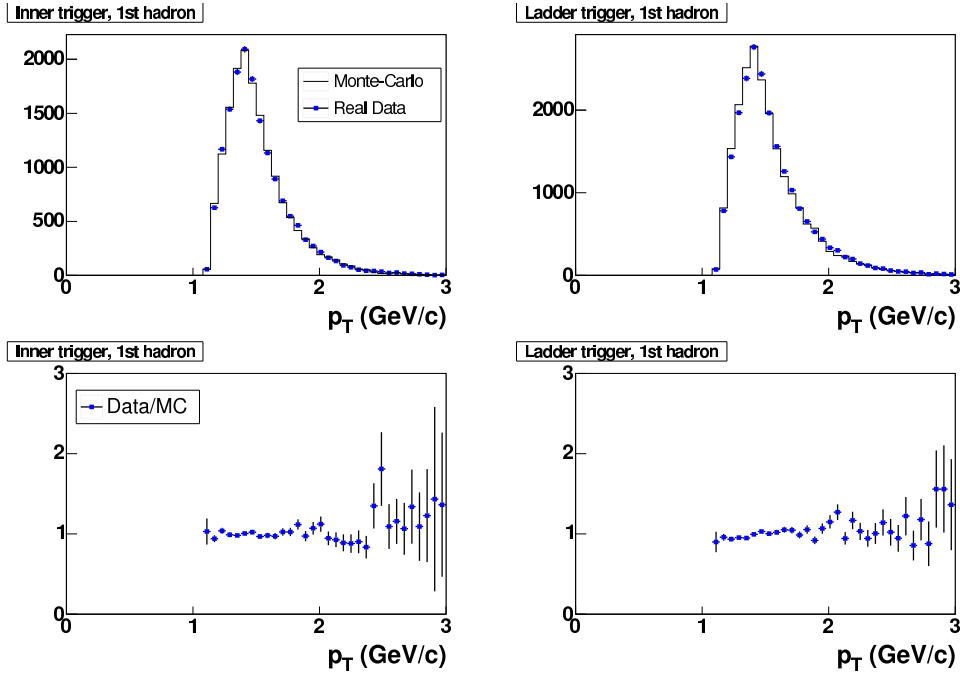


**Fig. 8.** Comparison of data and MC for the high  $p_T$   $Q^2 < 1$   $(\text{GeV}/c)^2$  sample. The upper plots present  $p_T$  distribution of leading hadron for two selected triggers. On the bottom plots the ratio data/MC is presented.

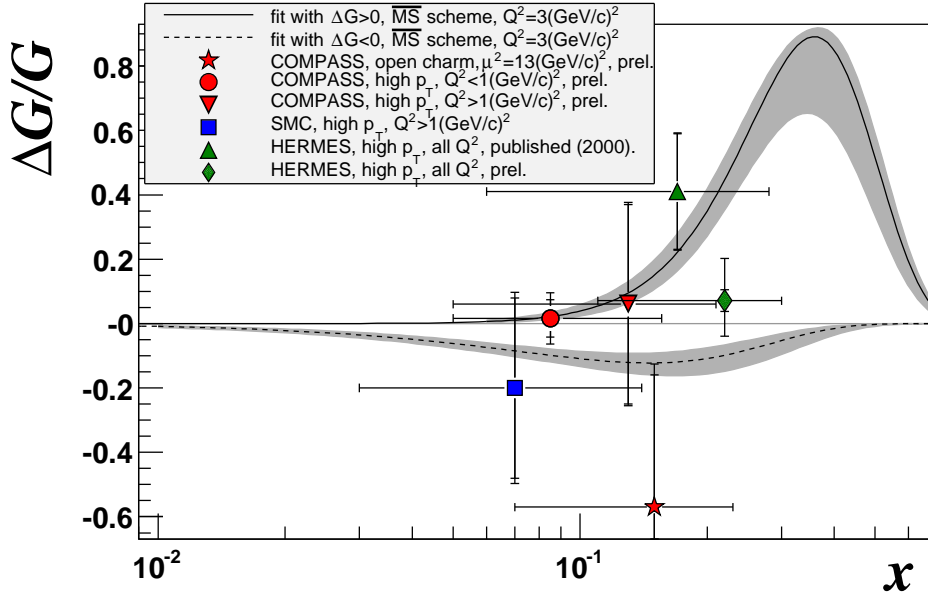


**Fig. 9.** Comparison of the  $\Delta G/G$  measurements from COMPASS, SMC [24] and HERMES [25]. For each point, vertical error bars indicate statistical and systematical uncertainty. Horizontal bars represent the corresponding  $x_g$  range. Lines were obtained from NLO QCD fits including COMPASS deuteron results on  $g_1^d$  [6]. Two equally good solutions for  $\Delta G/G$  were found. For both fits  $|\Delta G| = 0.2 - 0.3$  is obtained.